Flow Measurement and Instrumentation 62 (2018) 176–185

Contents lists available at ScienceDirect

Flow Measurement and Instrumentation

journal homepage: www.elsevier.com/locate/flowmeasinst

Liquid distribution and holdup in the random packed column

A.F. Velo*, D.V.S. Carvalho, M.M. Hamada

Instituto de Pesquisas Energéticas e Nucleares – IPEN/CNEN-SP, Av. Prof. Lineu Prestes, 2242 Cidade Universitária, 05508-000 São Paulo, Brazil

ARTICLE INFO

Keywords:
Random packed column
Holdup
Multiphase systems
Industrial computed tomography
Phases distribution

ABSTRACT

In the present work, a third-generation gamma transmission tomography system was used to evaluate the liquid distributions of a Raschig rings random packed column, at two different water flows: 2 and 6 l/min. For each water flow, the measurements were carried out at nine column heights. The liquid-gas holdup was determined by the reconstructed images. The distribution of the Raschig rings, as well as the position and the average accumulated amount of the water concentration among the Raschig rings were capable to be determined, even at low temporal resolution of the system of 8.8 h. The regions of accumulated water concentration were similar for the water flow velocities at 2 and 6 l/min. The average accumulated water concentration for 6 l/min was higher compared to 2 l/min. The spatial resolution of the tomography system determined by the modulation transfer function (MTF) analysis was of 1.45 mm.

1. Introduction

Random packed distillation columns are used extensively in chemical and petrochemical industries to perform highly efficient process separation. With the recent advances in computational fluid dynamics, it is now possible to model the effects of heterogeneities in the bed on flow profiles and, hence, on the mass transfer efficiency [1–3]. Liquid flow distribution has been a major concern when scaling up random packed columns. The liquid distribution in random packed columns is not often uniform, even if the liquid is uniformly introduced into the column [4]. The knowledge on porosity variation (gas holdup) of random packed columns is useful for understanding the fluid dynamics [5,6]. The porosity variation in the random packed columns has long been recognized as a potential source of maldistribution and it has been studied extensively. Little information is available on modern high efficiency packings like stainless steel Raschig rings. Chu & Ng [7] and Mc Greavy et al. [8] showed that the porosity distribution has a significant effect on the liquid flow distribution within a packed column near the wall region. Non-uniform distribution of porosity results in liquid flow maldistribution and a reduced separation efficiency.

From the mid-80, the description of the first works using non-destructive methods, such as computed tomography and X-ray range, may be found in the literature. Niu et al. [9] used the X-ray computed tomography to analyze the radial porosity distribution in a bed of randomly packed uniform spheres and observed oscillations in the porosity distribution in the radial direction. Chaouki & Dudukovic [5] and Chen et al. [10,11], measured the porosity distribution in random packed beds with gamma ray computed tomography. Toye et al. [12] used the X-ray computed tomography to measure the porosity distribution and liquid holdup in complex packed beds widely used in distillation and absorption. All these results showed that, for the packings with complex geometrical shapes, the porosity distribution in packed beds was non-uniform and the radial variation did not show oscillatory patterns, such as those found for spheres.

Yin et al. [4] studied the liquid (water) holdup distribution in a large scale packed column filled with metal Pall rings, using non-invasive gamma ray tomography technique. It was found that the liquid holdup distribution was not uniform and that the liquid distributing design had a significant effect on the holdup distribution. Vasquez et al. [3] studied the porosity distribution in a column randomly packed with three different sizes of stainless steel Raschig rings with the gamma ray scanner at L/D = 2 plane, where L and D is the length and the diameter of the column. They demonstrated that the spatial porosity distribution in random packed columns is not uniform and, for the circumferentially averaged radial porosity distribution, the porosity in the column wall region tends to be higher than that in the bulk region, due to the effect of the column wall.

Schubert et al. [13] studied the solid patterns and the liquid distribution in a 300 mm diameter column packed with a metal Pall Rings. Both measurements were carried out using a tomography system comprising 320 lutetium-yttrium-orthosilicate (LSYO) detectors, each one of 2 mm × 8 mm active area and a collimated isotopic ^{137}Cs, with a 44° fan beam. The Pall Rings were arranged in three sections: (a) random packing, (b) horizontal layer and (c) in upright orientation. The

* Corresponding author.
E-mail address: afvelo@ipen.br (A.F. Velo).

https://doi.org/10.1016/j.flowmeasinst.2017.11.002
Received 10 May 2017; Received in revised form 28 September 2017; Accepted 6 November 2017
Available online 08 November 2017
0955-5986/ © 2017 Elsevier Ltd. All rights reserved.

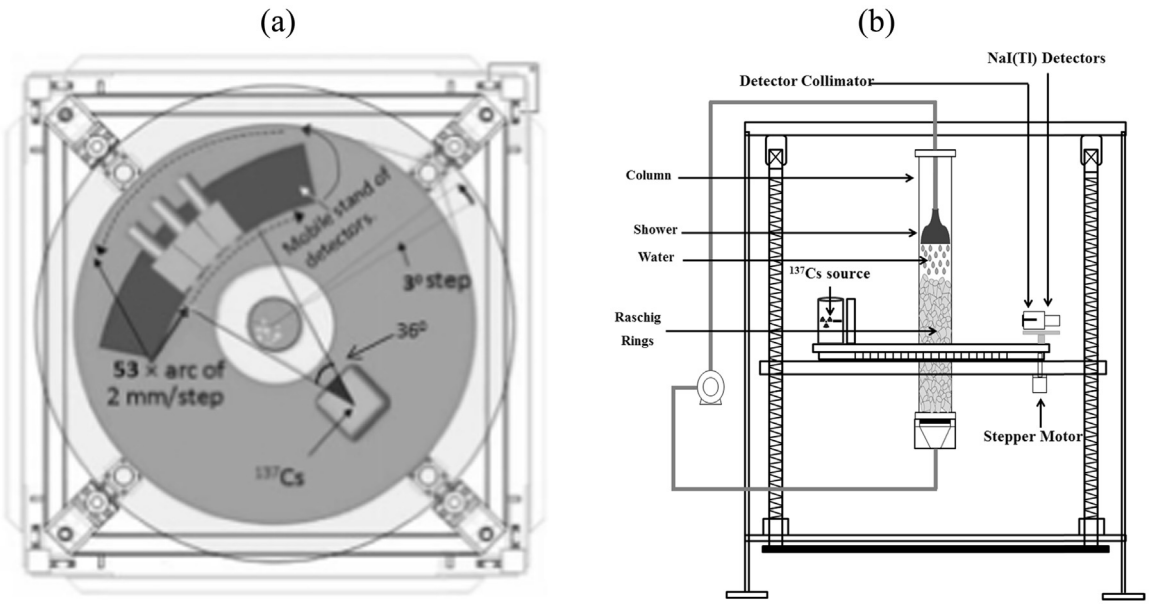

Fig. 1. Diagram of the third generation CT scanner used. (a) Top view and (b) side view.

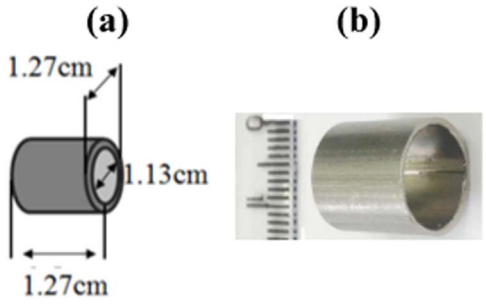

Fig. 2. Scheme (a) and picture (b) of the metal Raschig rings.

tomography measurements were performed only in a single layer. The differences in solid patterns, as well as the liquid distribution were clearly visualized with the tomography used. Loane et al. [14] showed experimentally that the gas superficial velocity does not influence the liquid hold up in an open-structure random packed column with counter current flow, contrary to what is observed for more conventional packings. The liquid hold up is determined only by liquid superficial velocity and a simple correlation is proposed.

In the present work, a third-generation gamma transmission tomography system was used to evaluate the gas and liquid distributions at two different water flows: 2 and 6 l/min in the random packed column filled with Raschig rings. For each water-flow, the measurements were

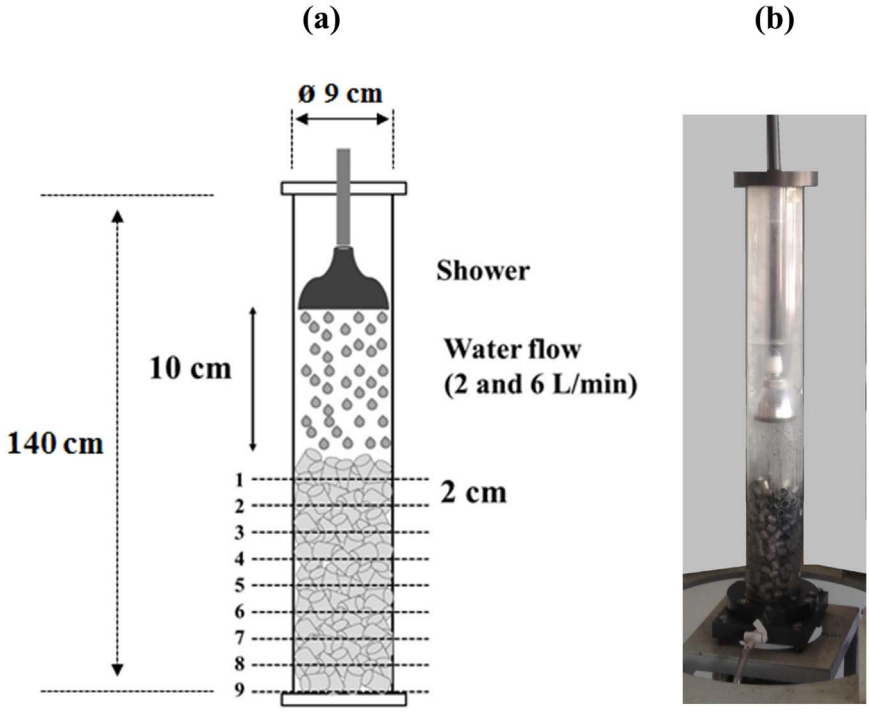

Fig. 3. Scheme (a) and picture (b) of the experimental random packed column.

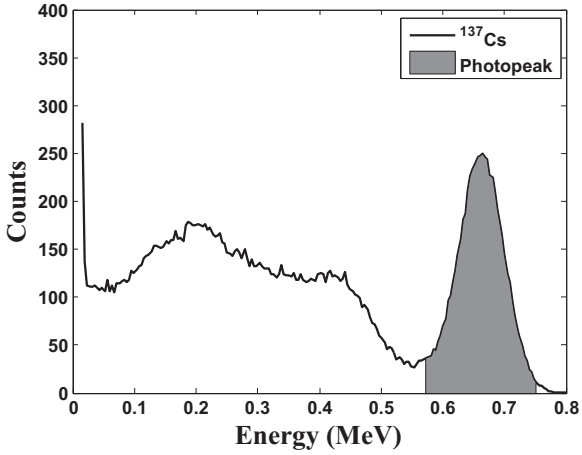

Fig. 4. ^{137}Cs Spectrum with the photopeak crosshatched selection.

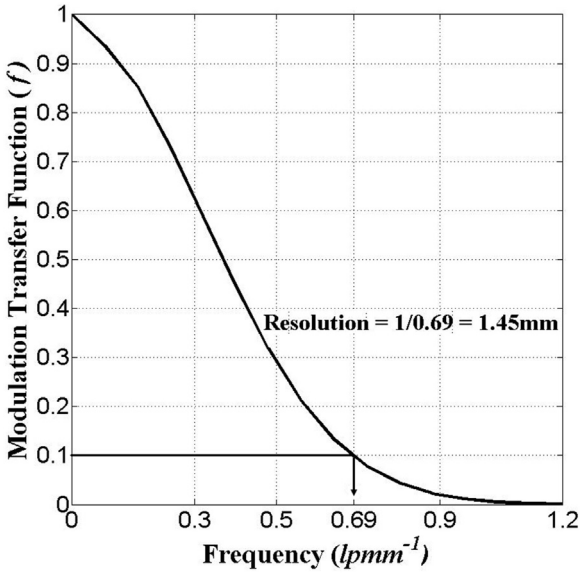

Fig. 5. Modulation transfer function analysis for the image reconstruction.

carried out at nine column heights.

2. Material and methods

A third generation computed tomography system, comprising three NaI(Tl) detectors of 50 × 50 mm^2 (diameter, thickness) shielded with lead, was used. The detectors were placed on a gantry in fan-beam geometry opposite to the gamma ray source, as shown in Fig. 1. The three NaI(Tl) detectors were individually collimated with lead containing a septa of 2 × 5 × 50 mm^3 (width, height, depth). The detectors move 53 times in a step angle of 0.226 degree, emulating 159 detectors per projection. The counting time for sampling was 5 s. Thereafter, the support table containing the gantry and the ^{137}Cs gamma source (Fig. 1) rotates three degrees forward, and this process goes on up to completing 360 degrees, totalizing 120 projections. For a total of 19080 samples (159 'virtual detectors' × 120 projections) the system spends 31800 s or 8.8 h to obtain each tomography image. The ^{137}Cs radioactive source, with an activity of 3.0 GBq (81 mCi), was placed into a radioactive shield-case with an aperture angle of 36 degrees (Fig. 1). This system was previously described by Mesquita et al. [2,15].

The column containing Raschig rings, randomly arranged, was placed in the center of the tomography system. The column was a Perspex cylindrical tube of ρ ≅ 1.2 g/cm^3 density, $\varnothing_{int}$ = 8 cm internal diameter, $\varnothing_{ext}$ = 9 cm external diameter (0.5 cm wall thickness) and column height, h = 140 cm. The Raschig rings are composed of stainless steel with external diameter of 1.27 cm, internal diameter of 1.13 cm and length of 2.5 cm (Fig. 2). Inside the column and 10 cm above the random Raschig rings column (Fig. 3), a shower was coupled with the intention of obtaining a well-distributed water flow throughout the entire inner column area. Experiments were carried out using two different water flows, one set at 2 l/min and the second set at 6 l/min. For each water flow experiment, nine tomography measurements were carried out, beginning from the top of the Raschig rings column and decreasing in steps of 2 cm (Fig. 3).

The statistical algorithm maximum likelihood estimation method (MLEM) was used to reconstruct the tomography images. The matrix of the P values in Eq. (1), i.e., the logarithmic of the ratio I_0/I were used as MLEM input data. I_0 refers to the values of tomography measurements without water flow and I is assigned to the tomography measurements with the water flow.

$$P = \ln\left(\frac{I_0}{I}\right) \tag{1}$$

Using the Eq. (1), Raschig ring pieces do not appear in the reconstruction image. In this manner, it is possible to infer the proportion of the water and air at each pixel using the matrix system of the Eq. (2) [3]. This procedure is only valid if the Raschig rings do not move during tomography measurements.

$$\begin{bmatrix} c_{i,j}^{W} \\ c_{i,j}^{A} \end{bmatrix} = \begin{bmatrix} \mu_W^E & \mu_A^E \\ 1 & 1 \end{bmatrix}^{-1} \cdot \begin{bmatrix} \mu_{i,j}^E \\ 1 \end{bmatrix} \tag{2}$$

In Eq. (2), for a specific energy ***E***, μ_W^E and μ_A^E are the theoretical linear attenuation coefficients (cm^{-1}) for water (W) and air (A), respectively [16]. $\mu_{i,j}^E$ is the experimental linear attenuation coefficient obtained from the reconstructed image at (i,j)th pixel. $c_{i,j}^W$ and $c_{i,j}^A$ are the holdup of the water and the air in the (i,j)th pixel, respectively.

The data provided by the holdup may be analyzed measuring the holdup average values in concentric circular radial intervals (azimuthal average). The radial holdup ε(r) is obtained by Eq. (3) [17,18].

$$\varepsilon(r) = \frac{1}{2\pi}\int_0^{2\pi} \varepsilon(r, \theta) d\theta \tag{3}$$

Both tomography measurements of I and I_0 (Eq. (1)), used to reconstruct the images, were obtained at the photopeak area of the ^{137}Cs spectrum [3,18], as showed in Fig. 4.

Fourier based methodology is a prevalent approach to characterize imaging performance. This includes the modulation transfer function (MTF), which characterizes the spatial resolution of the imaging system [19,20]. The MTF analysis was carried out in order to obtain the spatial resolution of the tomography system. In the present work, the MTF was calculated using the Edge Spread Function, commonly known as ESF parameter [21]. One advantage of using the MTF is that this methodology provides quantitative values of the spatial resolution along all the frequency range. Conventionally, the maximum spatial resolution is estimated as the inverse of the value at 10% of MTF curve [21,22].

3. Results and discussion

The MTF is the scientific means of evaluating spatial resolution

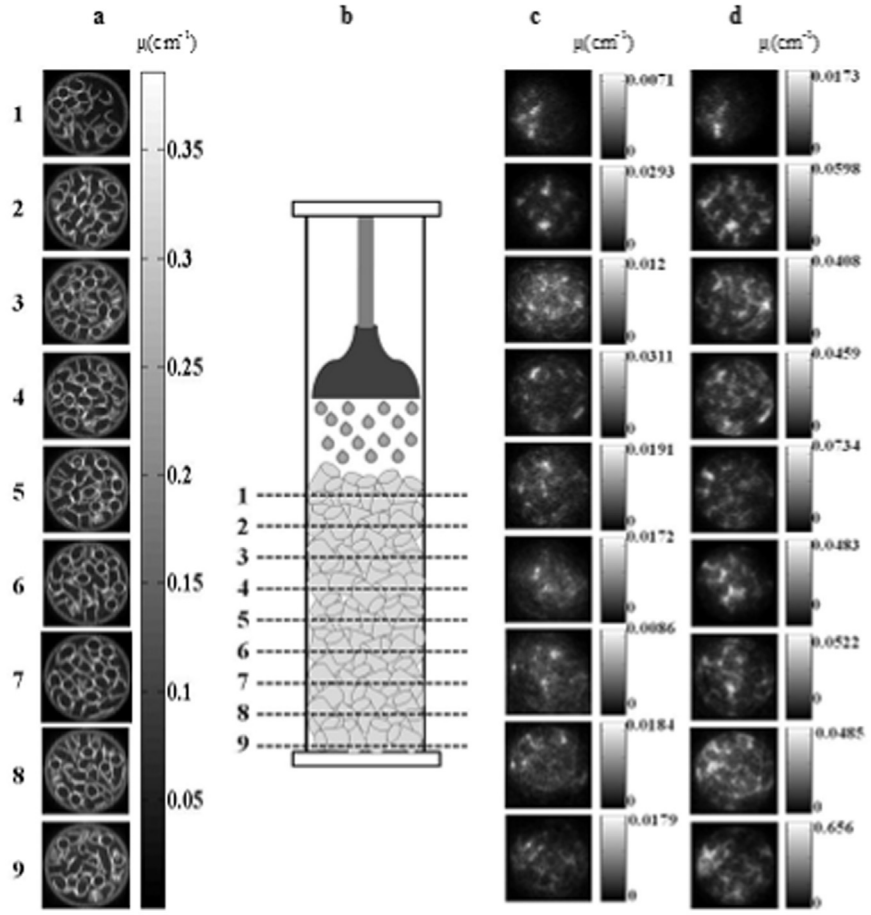

Fig. 6. Reconstructed images without water flow (a); column scheme (b); reconstructed images with water flow of 2 l/min and reconstructed images with water flow of 6 l/min.

performance of an imaging system; and infers how well the system transfers contrast across spatial frequencies, which is an advantage of this methodology [19,20]. This parameter could be considered a guide to choose the tomography system to carry out an experiment like the present study, since the spatial resolution can be estimated before carrying out tomography measurements, informing previously if the parameters selected for scanning are suitable. In other words, a spatial resolution of at least the Raschig rings thickness value is required for such an experimental investigation by means of gamma ray tomography. The spatial resolution of the tomography system, analyzed by MTF was 1.45 mm, what is very close to the Raschig ring thickness used (1.4 mm). Fig. 5 presents the curve which estimated the tomography system spatial resolution. However, the temporal resolution, another parameter for gamma ray tomography system, is low, i.e., the time necessary to obtain an image is relatively long.

The tomography measurements carried out at nine different heights of the random packet column are shown in Fig. 6. Fig. 6(a) comprises the reconstructed images of the Raschig rings column at nine heights, without water flow. As it may be observed, a high spatial resolution was obtained with the selected parameters. The color-bar for these images has the same index, where the index value represents the linear attenuation coefficient ($\mu(cm^{-1})$). Fig. 6(b) is the scheme of the column illustrating the nine tomography measurement positions. In Fig. 6(c) and 6(d), the reconstructed images for water flow of 2 and 6 l/min are shown, respectively. These images were reconstructed using Eq. (1), where, Io corresponds the Raschig rings column without water flow and I is the same column with water flow (2 and 6 l/min). The reconstructed images obtained from this procedure shows that the Raschig rings did not moved during the measurements, since the images observed in Fig. 6(c) and 6(d) are only the proportion of accumulated water and air in each pixel and no ring was detected. This phenomenon may be due to the high density of the stainless steel, which is around 8 g/cm^3.

The results of the reconstructed images (Fig. 6(c) and 6(d)) suggest that higher accumulated water concentrations are found in the same regions for both water flows: 2 and 6 l/min. For 6 l/min water flow, higher water concentration regions may be observed more easily. One caution to be taken in the analysis of the tomography images is the significance of the index for each pixel in the figure. The range of the pixel index may be inferred from the color bar of Fig. 6. If the pixel index is low, it means that the water concentrations are low. For example, the image of the sampling #6 (Fig. 6(c)) shows two higher brightness regions, suggesting that the average accumulated water concentration in those two positions could be high. However, as illustrated by the color bar (maximum 0.0071), the amount of water in these two bright regions is very low, once the linear coefficient attenuation of the water is 0.08574 for 662 keV energy.

In Fig. 7, the overlapping of Fig. 6(a) with Fig. 6(c) and Fig. 6(a) with Fig. 6(d), is shown, where the blue color represents the average accumulated water concentration. As it may be inferred from Fig. 7, it was possible to visualize, clearly, the region where the water concentration is accumulated among the Raschig ring edges, since the amount of accumulated water concentration depends on the position

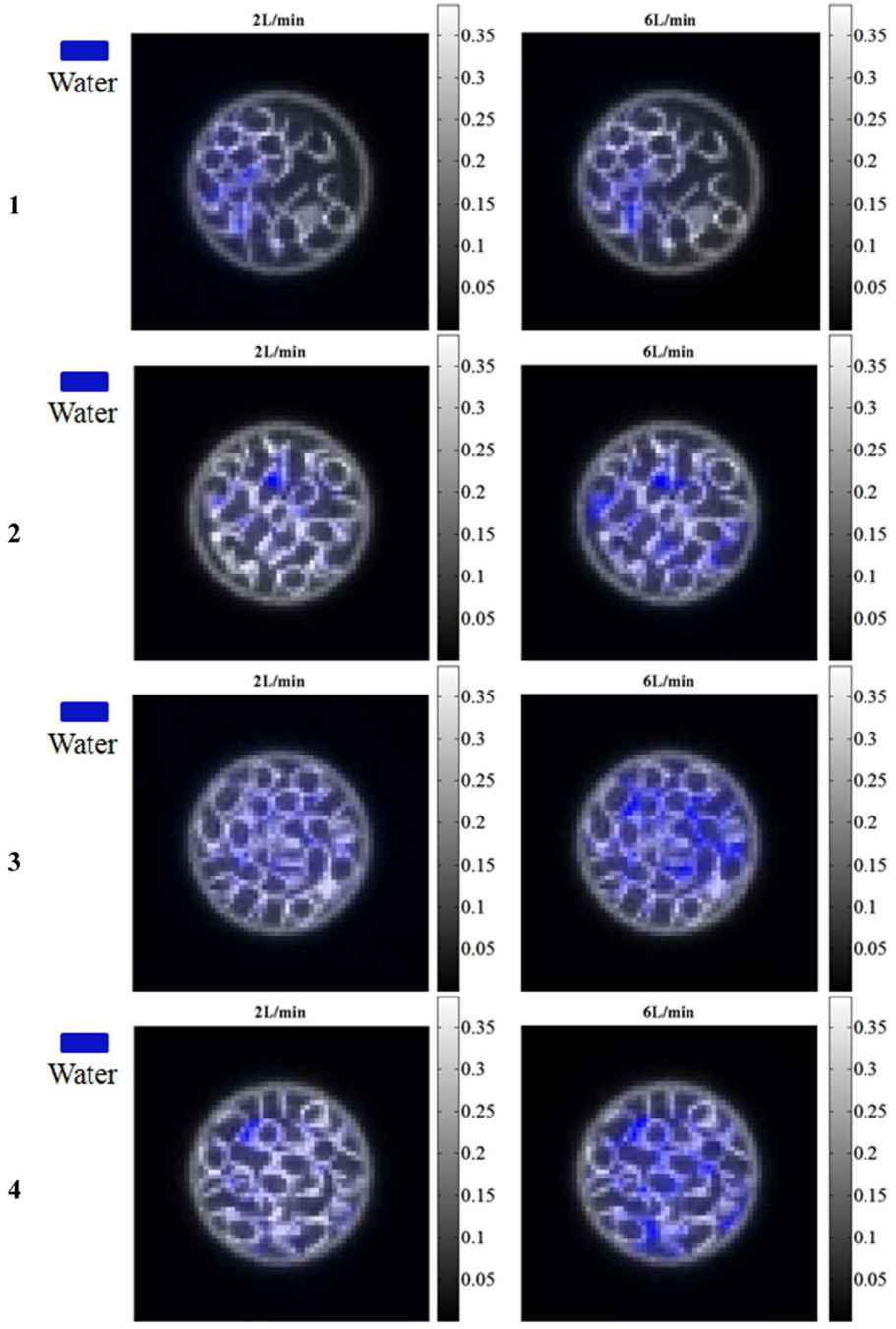

Fig. 7. Overlapping of Raschig rings without water, with the images of the water for 2 l/min and 6 l/min. The blue color represents the average accumulated water concentration.

and distribution of Raschig rings, as well as the water flux velocity.

Another way to analyze tomography results is to use the holdup analysis, as shown in Fig. 8. This type of analysis may provide the quantity of water (bottom) and gas (upper) at each pixel of the reconstructed image, as well as the spatial distribution of these materials. As showed in Fig. 8, region #2 shows the highest average accumulated water concentration reaching, in some pixels, the level of 70% (water holdup of 0.7) of water. On the other hand, the regions #6 and #7 for 2 l/min from Fig. 8 present low average accumulated water concentration due to the position of the rings that enables the flow of the water through the rings. However, increasing the water flux from 2 l/min to 6 l/min, a larger accumulated water concentration was found, probably, due to the inlet flow of the water is greater than the outflow of water. This phenomenon can be also observed in Fig. 7.

In our tomography system used, due to its low temporal resolution of 8.8 h, it was possible to measure only the average accumulated water concentration in the Raschig rings edges. Also, the water flow that passes freely among the Raschig rings could not be measured, because its thin thickness was not able to attenuate the high energy beam from 662 keV ^{137}Cs source, used to comprise the tomography system.

As expected, a close cross-sectionally symmetrical distribution was obtained because the system has low temporal resolution (8.8 h) and,

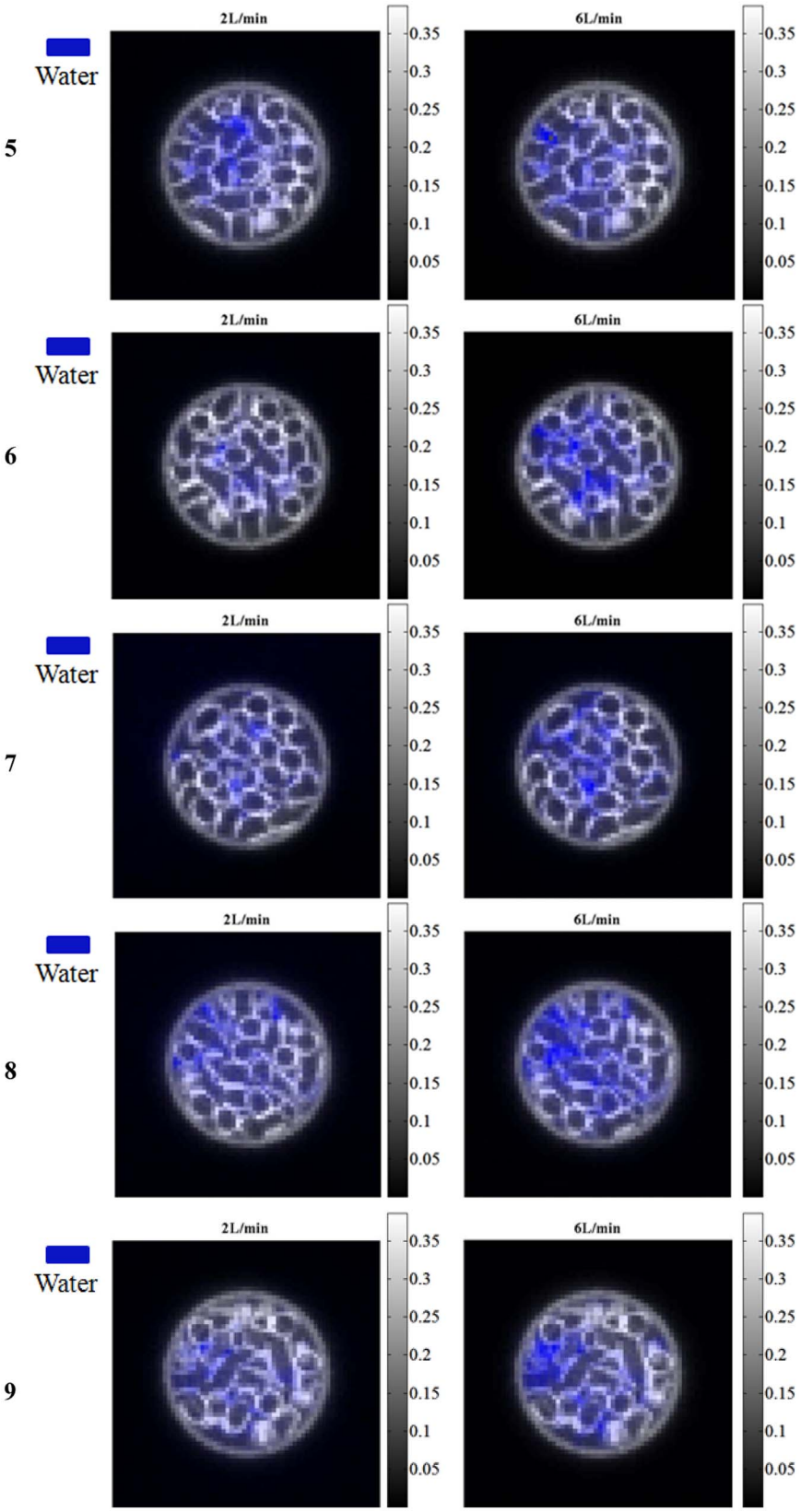

Fig. 7. (*continued*)

therefore, it provides only a time averaged distribution of the holdup images. This symmetrical distribution may be observed by the holdup average values in concentric radial intervals (ε(r)), presented in Fig. 9. Additionally, from the Figs. 8 and 9, it can be inferred for all heights the holdup values maintain a similar tendency for both flow, i.e. 2 and 6 l/min. This tendency can be visualized in the Fig. 10 that illustrates the area under the curve of the radial holdup values (ε(r)) obtained in Fig. 9.

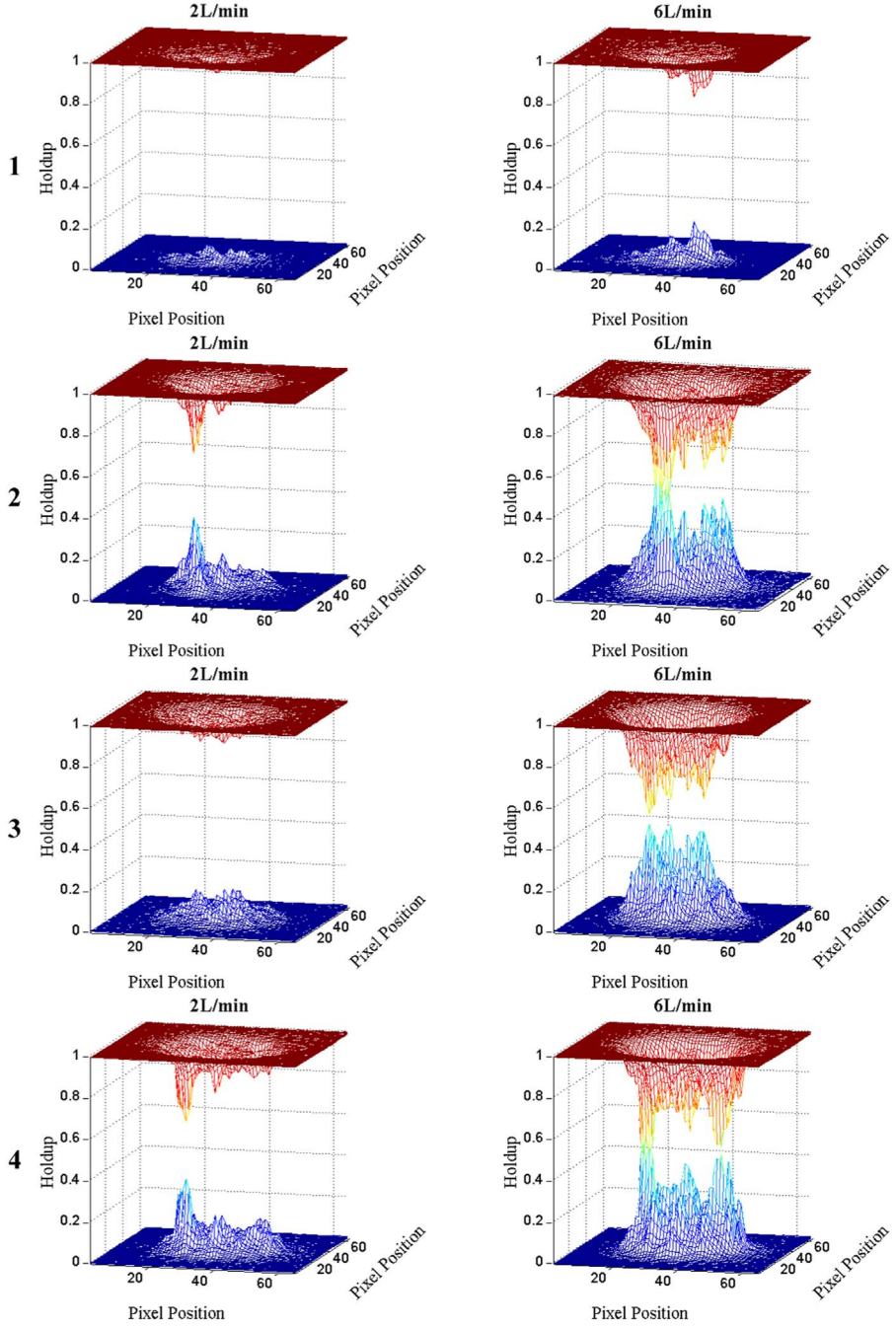

Fig. 8. Holdup of air (top) and water (bottom) at different positions of Raschig ring column.

These results demonstrated that the random packed column has a good uniformity in the water distribution, providing larger contact between the water and the Raschig ring surface. For industrial processes, it is important that the product present high surface contact and a uniform water distribution.

4. Conclusion

The tomography system spatial resolution used in this paper, determined by the modulation transfer function (MTF), was 1.45 mm, very close to the Raschig ring thickness used (1.4 mm). This result meets the requirement that the spatial resolution of the system should be smaller or at least close to the thickness of Raschig rings.

The regions of accumulated water concentration were similar for both water flow velocities, i.e., 2 and 6 l/min (Fig. 7), as expected. However, the average accumulated water concentration for 6 l/min was higher compared to 2 l/min, due to the fact that the water flow inlet is higher than the water flow outlet. This behavior may be observed by the index of color bar from Fig. 6(c) and (d), as well by the holdup values from Fig. 8(a) and (b).

The symmetrical distribution was obtained by the holdup average values in concentric radial intervals (ε(r)) due to the low temporal

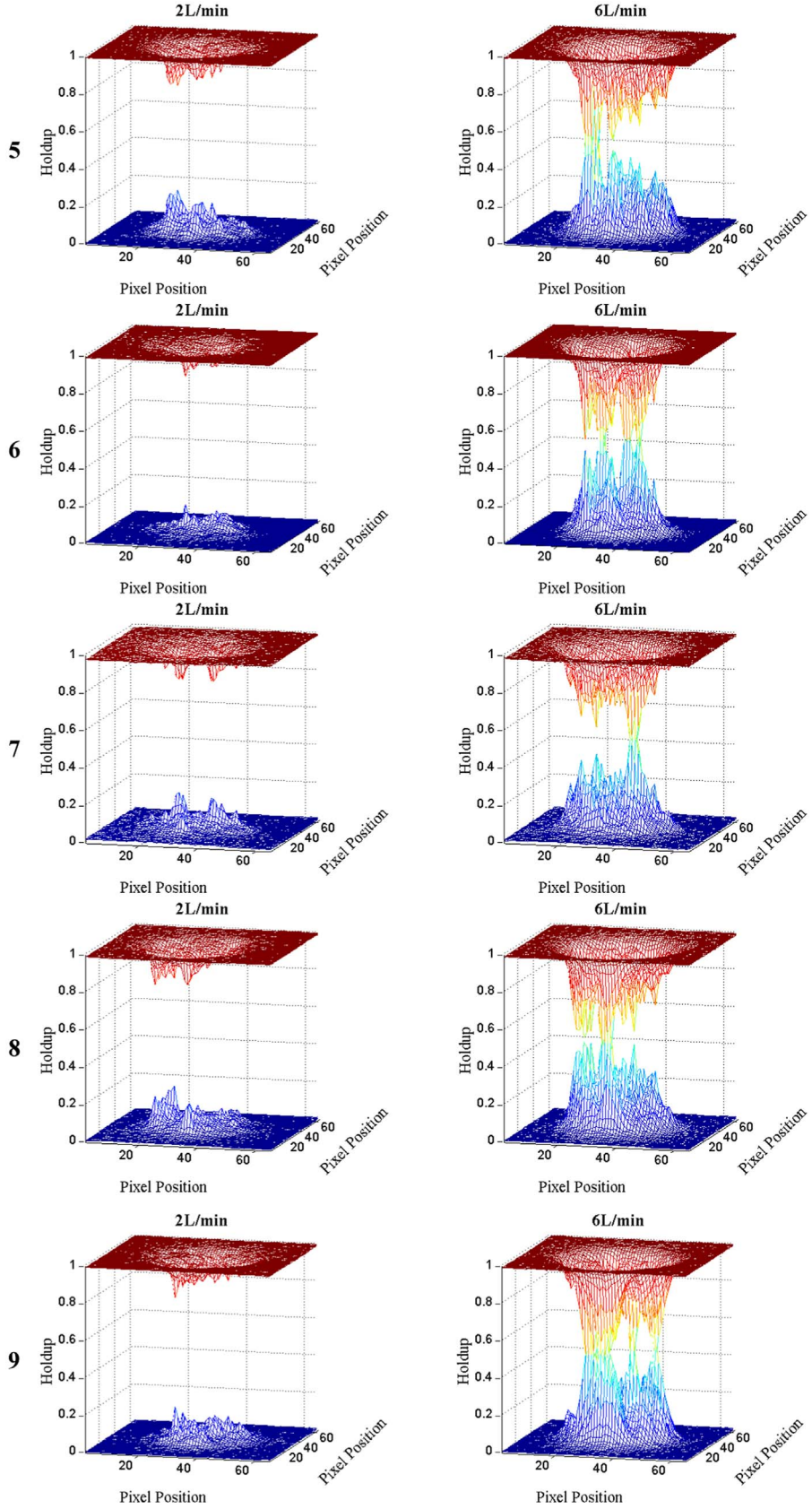

Fig. 8. (*continued*)

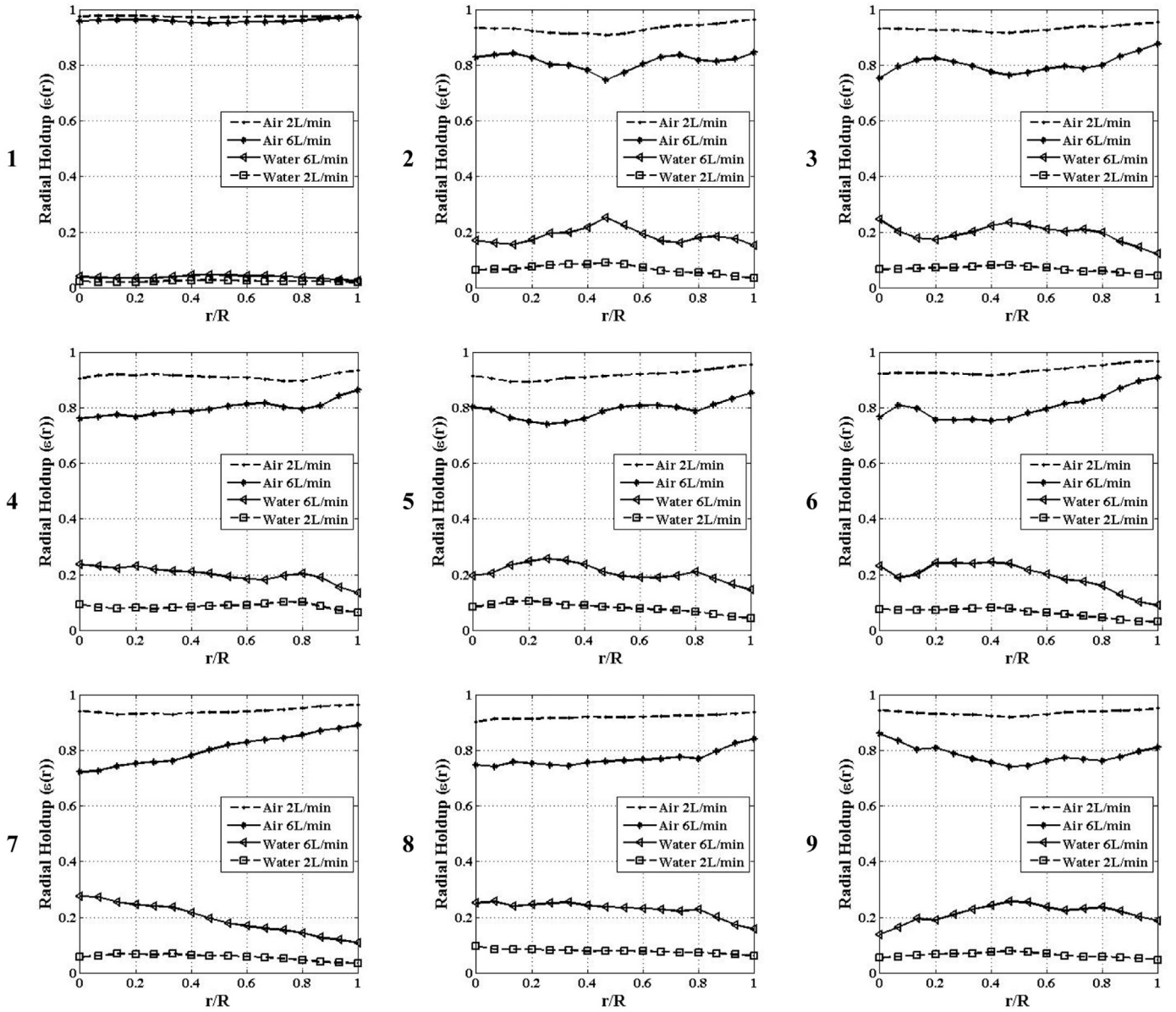

Fig. 9. Radial holdup (ε(r)) for nine heights analysis.

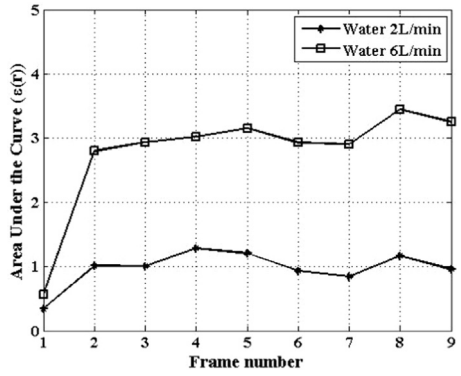

Fig. 10. Liquid phase area under the curve of the radial holdup (ε(r)).

resolution of the tomography system used (Fig. 9).

These results demonstrated that the tomography system used in this work is able to evaluate the position and the amount of the water concentration and the distribution of the Raschig rings, even at low temporal resolution of the system. It should be emphasized that the Raschig rings did not move during the measurements because of their high density stainless steel.

Acknowledgments

The authors would like to express their gratitude to CNPq (The Brazilian National Research Council Grant nos. 305210/2013-0 and 308560/2015-9) and FAPESP (Foundation for Research Support of the State of São Paulo Grant number 2012/22705-3) for financial support and fellowship.

References

[1] Z. Wang, K. Afacan, K. Nandakumar, K. Chuang, Porosity distribution in random packed columns by gamma ray tomography, Chem. Eng. Proc. 40 (2001) 209–219.
[2] C.H. Mesquita, A.F. Velo, D.V.S. Carvalho, M.F.T. Martins, M.M. Hamada, Industrial tomography using three different gamma ray, Flow Meas. Instrum. 471 (2016) 1–9.
[3] P.A. Vasquez S, C.H. Mesquita, G.A.C. LeRoux, M.M. Hamada, Methodological analysis of gamma tomography system for large random packed columns, Appl. Radiat. Isot. 68 (2010) 658–661.
[4] F. Yin, Z. Wang, A. Afacan, K. Nandakumar, K.T. Chuang, Experimental studies of

liquid flow maldistribution in a random packed column, Can. J. Chem. Eng. 78 (2000) 449–457.
[5] J. Chaouki, F. Larachi, M.P. Dudukovic, Noninvasive tomographic and velocimetric monitoring of multiphase flows, Ind. Eng. Chem. Res. 36 (1997) 4476–4503.
[6] S. Rabha, M. Schubert, M. Wagner, D. Lucas, U. Hampel, Bubble size and radial gas hold-up distributions in a slurry bubble column using ultrafast electron beam X-ray tomography, AIChE J. 59 (5) (2012) 1709–1722.
[7] C.F. Chu, K.M. Ng, Flow in packed tubes with a small tube to particle diameter ratio, AIChE J. 35 (1989) 148–156.
[8] C. Mc Greavy, E.A. Foumeny, K.H. Javed, Characterization of transport properties for fixed bed in terms of local bed structure and flow distribution, Chem. Eng. Sci. 41 (1989) 787–797.
[9] M. Niu, T. Akiyama, R. Takahashi, Yagi, Reduction of the wall effect in a packed bed by hemispherical lining, AIChE J. 42 (1996) 1181–1186.
[10] J. Chen, N. Rados, M.H. Al-Dahhan, M.P. Dudukovic, D. Nguyen, K. Parimi, Particle motion in packed/ ebullated beds by CT and CARPT", AIChE J. 47 (5) (2001) 994–1004.
[11] J.W. Chen, P. Gupta, D. Sujatha, M.H. Al-Dahhan, M.P. Dudukovic, B.A. Toseland, Gas holdup distribution in large diameter bubble columns, Flow Meas. Instrum. 9 (2) (1998) 91–101.
[12] D. Toye, P. Marchot, M. Crine, Local measurements of void fraction and liquid holdup in packed columns using X-ray computed tomography, Chem. Eng. Proc. 37 (1998) 511–520.
13] M. Schubert, A. Bieberle, F. Barthel, S. Boden, U. Hampel, Advanced tomographic techniques for flow imaging in columns with flow distribution packings, Chem. Ing. Tech. 83 (7) (2011) 1–14.
[14] L.P.M. Loane, J.C. Schouten, J. van der Schaaf, Pressure drop and liquid hold up in an open-structure random packed column with counter current flow, In: 2016 AIChE Annual Meeting Proceedings. November 13-18, 2016, São Francisco, CA, USA.
[15] C.H. Mesquita, D.V.S. Carvalho, R. Kirita, P.A.V. Salvador, M.M. Hamada, Gas–liquid distribution in a bubble column using industrial gamma-ray computed tomography, Rad. Phys. Chem. 95 (2014) 396–400.
[16] The National Institute of Standards and Technology (NIST) The Physical Measurement Laboratory (PML), ⟨http://physics.nist.gov/PhysRefData/Xcom/html/xcom1.html⟩, Visited at August 2015.
[17] A. KEMOUN, B. CHENG ONG, M.P. DUDUKOVIC, Gas holdup in bubble columns ate elevated pressure via computed tomography, Int. J. Multiph. Flows 27 (2001) 929–946.
[18] S.B. KUMAR, Tomographic measurements of void fraction and modelling the flow in bubble columns, Ph.D. Thesis, Washington University, St. Louis, 1994.
[19] S.L. Richard, D.B. Husarik, G. Yadava, S.N. Murphy, E. Samei, Towards task-based assessment of CT performance: system and object MTF across different re-construction algorithms, Med. Phys. 39 (2012) 4115–4122.
[20] E. Samei, M.J. Flynn, D.A. Reimann, A method for measuring the presampled MTF of digital radiographic systems using an edge test device, Med. Phys. 25 (1) (1998) 102–113.
[21] A.F. Velo, M.M. Hamada, D.V.S. Carvalho, J.F.T. Martins, C.H. Mesquita, A portable tomography system with seventy detectors and five gamma-ray sources in fan beam geometry simulated by Monte Carlo method, Flow Meas. Instrum. 53 (2017) 89–94.
[22] D.J. Dowsett, P.A. Kenny, R.E. Johnston, The Physics of Diagnostic Imaging, second ed, Hodder Arnold, 2006.